

# Preliminary Investigations of a Novel Dynamic CT Collimator

J. Webster Stayman<sup>a</sup>, Nir Eden<sup>b</sup>, Yiqun Q. Ma<sup>a</sup>, Grace J. Gang<sup>a</sup>, and Allon Guez<sup>c</sup>

<sup>a</sup>Biomedical Engineering, Johns Hopkins University, Baltimore, MD, USA

<sup>b</sup>Art Cybe, Kafr Saba, Israel

<sup>c</sup>Electrical and Computer Engineering, Drexel University, Philadelphia, PA, USA

## ABSTRACT

In this work we describe a new dynamic x-ray collimator that may be used to collect sparse computed tomography projection data. Data sparsity may be user-specified and controlled both angularly and radially - allowing a broad range of acquisition strategies. We consider protocols that have fully sampled projection data for a volume-of-interest with a sparsely sampled background. Model-based reconstruction methods are adapted to process the non-uniformly sampled projections. We demonstrate the ability of a CT system with this novel dynamic collimator to provide user controllable regional image quality and dose reduction in a set of phantom experiments.

**Keywords:** Dynamic Bowtie Filter, X-ray Modulation, Dose Reduction, Region-of-Interest Imaging

## 1. INTRODUCTION

Image quality and radiation exposure are closely related in x-ray computed tomography (CT). In general, higher exposures are used to produce higher quality images. This is particularly true when image quality is largely driven by quantum noise associated with the incident x-ray beam. Thus control over the intensity of x-ray beam provides an important control over the balance between radiation dose and image quality. Modern clinical CT systems provide control over the overall beam intensity through tube current modulation. Dynamic current control can be optimized to provide minimum noise variance in images.<sup>1</sup> The spatial distribution of fluence may also be shaped - typically through bowtie filters that attenuate the beam more at the periphery of the patient where less fluence is required. Current clinical systems often have the capability to select between a small number of static filters.

There have been many research efforts to construct modulators to permit dynamic control of the spatial distribution of the x-ray beam. Such devices are often described as dynamic bowtie filters and have taken many forms. Several designs based on variable beam attenuation have included actuated split filter designs, fluid-filled filters,<sup>2,3</sup> piece-wise linear filters with independently controlled leaves,<sup>4</sup> and grid-like structures that shape the beam based on angle of incidence.<sup>5</sup> Other designs have leveraged binary filters that block x-rays on a fine scale (below system resolution)<sup>6</sup> or that reduce fluence at a position based on dwell time.<sup>7,8</sup>

With the advent of advanced reconstruction algorithms, another widely researched strategy for altering the dose-image quality trade-off is sparse sampling. Angular undersampling has been widely explored and is straightforward to implement in pulsed cone-beam CT systems.<sup>9</sup> Combined angular and radial undersampling has been explored with the use of moving, structured collimators<sup>10</sup> and with alternate system geometries (e.g. a moving line detector with a pulsed source<sup>11</sup>).

Such dynamic beam control permits increased control over radiation dose and image quality. For example, the beam profile may be dynamically controlled to avoid radiation sensitive organs or to provide a customized regional dose deposition.<sup>12</sup> Customized regional image quality may also be specified or optimized for particular imaging tasks or anatomical locations.<sup>13</sup> This includes specialized volume-of-interest (VOI) scans that focus on a particular organ or region (e.g. cardiac, spine, etc.). With some acquisition approaches, only a small region-of-interest is exposed leading to increased complexity in data processing/local tomography due to truncated

---

Further author information: (Send correspondence to web.stayman@jhu.edu)

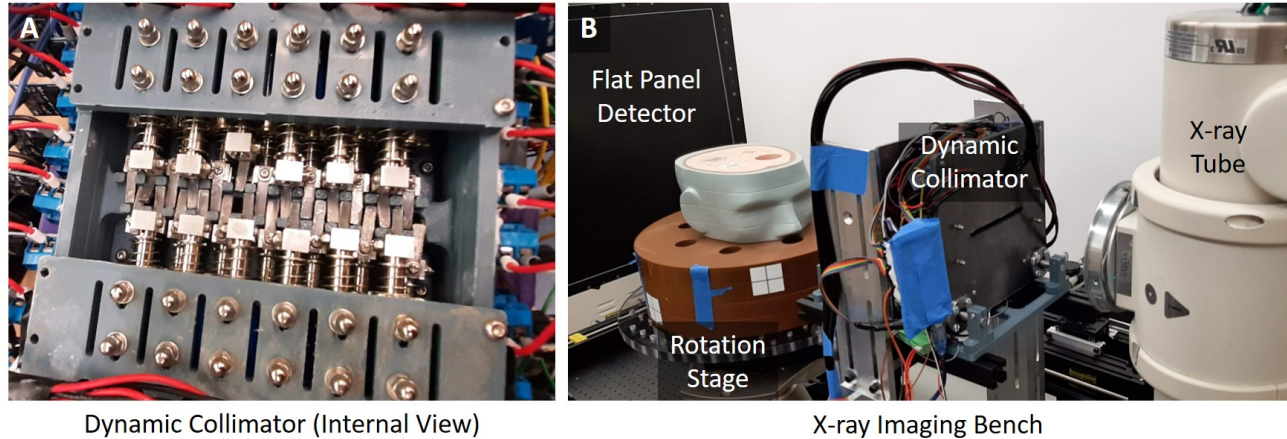


Figure 1. (A) Photograph of the fabricated dynamic collimator with 26 independently controlled blockers. (B) Integration of the dynamic collimator on an experimental x-ray imaging test-bench.

projections. Other approaches are able to provide very low exposure outside the VOI avoiding full truncation of projection data.

This work considers a new dynamic modulator that incorporates many of the ideas mentioned above. Specifically, the device uses a multitude of individually actuated "fingers" that locally block the x-ray beam. This enables various acquisition protocols including a fully sampled VOI surrounded by a background with angularly and radially sparse projection data. In this paper we describe the construction of the device and its installation in an x-ray imaging test-bench. Model-based image reconstruction is adapted and applied to the sparse projection data acquired from the experimental bench in two phantom experiments.

## 2. METHODS

### 2.1 Dynamic Collimator Design and Integration

A photograph of the proposed dynamic collimator is shown in Figure 1A. The device consisted of 26 independently actuated beam blockers. Each "finger" is made of a lead compound and is approximately 3 mm wide and 1.5 mm thick. This thickness stops  $> 99\%$  of x-rays to provide a nearly binary beam profile. The blockers are connected to a linear solenoid which is computer controlled. The array of blockers is contained in a 3D-printed housing with a lead-shielded entrance and exit slot (approximately 6 mm in height) on either side of the housing.

The collimator was mounted on an experimental x-ray test-bench comprised of a flat-panel detector (Varex 4343CB, Salt Lake City, UT), a radiographic/fluoroscopic x-ray tube (Varex Rad-94, Salt Lake City, UT), and a motion stage (Physik Instrumente, Auburn, MA). The dynamic collimator was placed with the blockers at  $\sim 30$  cm from the x-ray focal spot. This permitted full lateral coverage of the 43 cm detector in a CT system with 785 mm source-to-axis distance and 1050 mm source-to-detector distance. The x-ray tube was fitted with 2.1 mm of aluminum and 0.2 mm of copper filtration without any bowtie filter.

Computer controls for the collimator have been developed and integrated within the x-ray test-bench so that blocker motion occurs (with rotary stage motion) between acquisition frames in a step-and-shoot acquisition. Control software permits arbitrary positioning of blockers (e.g. open or closed) for every projection frame.

### 2.2 Data Acquisition and Processing

While the dynamic collimator permits arbitrary actuation of each blocker over each data frame, in this work we have focused on fully sampling a VOI surrounded by an undersampled background. This acquisition should provide image quality within the VOI that is comparable to fully sampled data and (generally) lower image quality in the background. We note that the sparse background sampling should help to avoid the complexity of local tomography and fully truncated data. Moreover, even if the background is lower image quality, this provides additional context for clinical tasks that would be absent from fully truncated data.

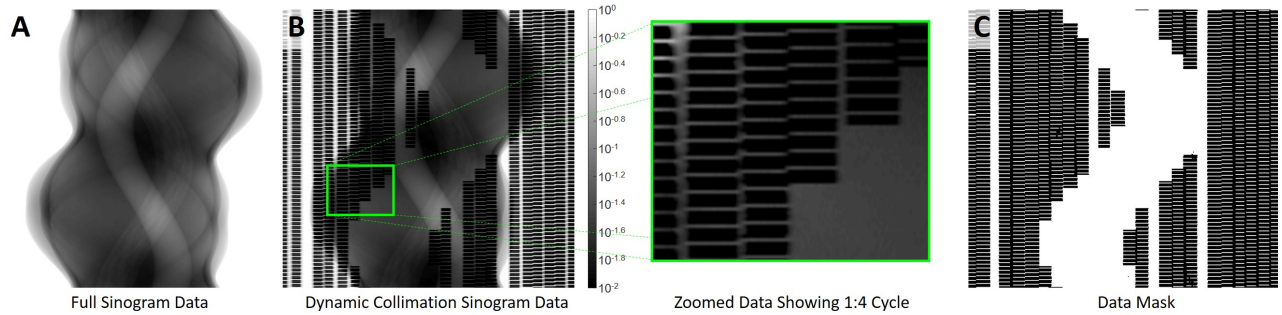


Figure 2. Illustration of fully sampled and dynamically controlled sampling. (A) Full sinogram data. (B) Dynamically collimated data with full sampling in an off-center VOI and 1:4 sampling outside the VOI. (C) A data mask generated for model-based reconstruction of the dynamically collimated data. (Note that there are four faulty blockers in this data which are stuck open.)

In these preliminary studies, we have opted to apply a duty cycle of 1:4 with respect to the background sampling. That is, outside the VOI, blockers were open for 1 frame followed by 4 closed frames. Moreover, open blockers were shifted frame-to-frame providing a combination of sparsity both angularly and radially. Thus, the exposure and sampling outside the VOI should be approximately 1/5 of the fully sampled case. This protocol for data collection is illustrated in Figure 2.

To reconstruct data acquired using this protocol, we used a modified penalized weighted least-squares (PWLS) reconstruction approach. Specifically, the mean measurement model was

$$\bar{y}(\mathbf{x}) = \mathbf{I}_0 \exp(-\mathbf{A}\mu), \quad (1)$$

where  $\mathbf{I}_0$  denotes the incident x-ray intensity,  $\mathbf{A}$  is the system matrix representing forward projection, and  $\mu$  denotes the vector of attenuation coefficients we wish to estimate. The PWLS objective is

$$\hat{\mu} = \arg \min_{\mu} \left( \mathbf{A}l - \mu \right)^T \mathbf{W} \left( \mathbf{A}l - \mu \right) + \beta \left\| \Psi \mu \right\| \quad (2)$$

$$l = -\log(y/\mathbf{I}_0) \quad (3)$$

where  $l$  denotes an estimate of the line integrals from the measurements  $y$ . The weighting matrix  $\mathbf{W}$  is a modified version of the standard PWLS weighting by the inverse of the variance. A total variation penalty with weighting  $\beta$  and first-order difference operator  $\Psi$  was applied.

To account for the sparse sampling pattern, a projection mask was estimated from a system gain scan. Specifically, the same actuation pattern was applied with no object in the scanner. A mask was formed using simple thresholding followed by a dilation operation to increase the size of mask. Dilation was applied only in the radial direction of the sinogram. A modified diagonal weighting matrix was formed such that  $\mathbf{W} = \mathbf{D}\{y \odot \text{mask}\}$ . In essence this informs the PWLS algorithm that blocked measurements should be ignored for reconstruction.

For all experiments in this work, a single central row of flat-panel data was used to form a sinogram. This projection data was comprised of 2x2 binned pixels (0.556 mm) and 360 projections. Reconstructions were formed using 200 iterations of the separable paraboloidal surrogates method<sup>14</sup> using 20 angular subsets and 0.75 mm voxels.

### 2.3 Physical Experiments

Two different physical experiments were conducted. Both use the system geometry and processing scheme described above. Acquisitions were conducted using an x-ray technique of 120 kVp and 20 mA. Exposures of 1 ms yield 0.02 mAs/frame. With 360 frames the total exposure was 7.2 mAs.

The first experiment used an ATOM head phantom (CIRS, Norfolk, VA) and two sampling strategies: 1) fully sampled data, and 2) the VOI plus 1:4 background sampling scheme described above. Data were reconstructed

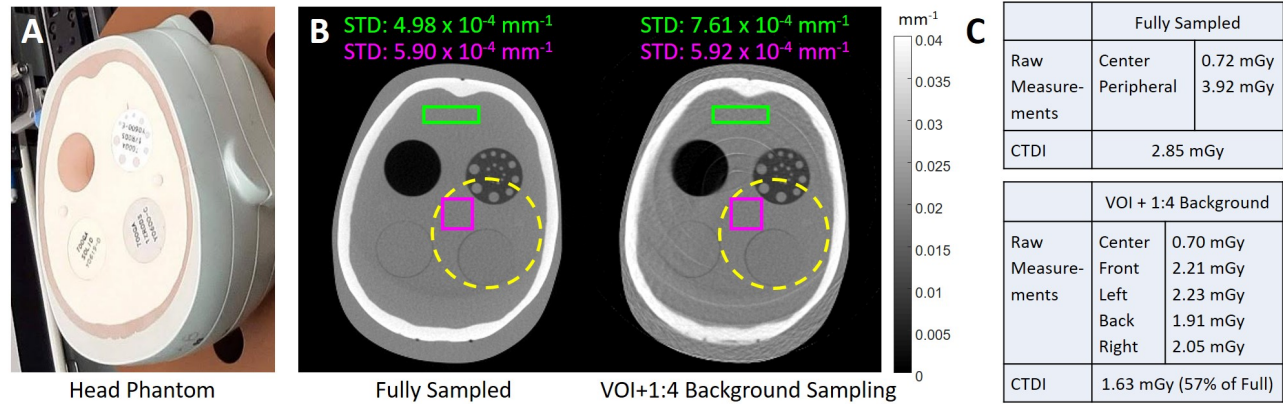


Figure 3. Summary of head phantom experiments. (A) Photograph of head phantom with three inserts. (B) Comparison of fully sampled and VOI+1:4 sparse sampling reconstructions. Two rectangular regions are identified over which sample noise variance is computed. The VOI is indicated by a dashed yellow circle. (C) Dose measurements for each acquisition protocol.

using the above processing with  $\beta = 1$  for fully sampled data and  $\beta = 1.3$  for the dynamically collimated data. Noise was measured at location both inside and outside the VOI.

Radiation dose was measured for each scan using a standard 16 cm CTDI head phantom and a 0.6 cc Farmer chamber (RadCal, Monrovia, CA). Center and peripheral dose was measured for the fully sampled scan, and all five dosimeter locations were used for the dynamically collimated scan. Total dose was computed using 1/3 center plus 2/3 peripheral averages.

A second experiment was performed using a thorax phantom (Kyoto Kagaku, Japan). Both fully sampled and dynamically collimated data were acquired. A VOI around the spine was selected and scanned using the VOI plus 1:4 sparsity as well as a VOI plus 2:4 sparsity. The latter method used open pairs of adjacent blockers.

### 3. RESULTS

Results of the head phantom experiment are summarized in Figure 3. Note that within the circular VOI the noise levels (as computed in the region identified by the magenta square) are nearly identical suggesting a very similar level of image quality. Outside the VOI, the noise levels (computed in green rectangle) are approximately 1.5 times higher in the VOI scan. We also note some ring artifacts associated with the boundaries of the blockers. We conjecture that this is the result of incomplete gain correction, gaps in radial sampling due to overlap of blockers (e.g. a whole column of missing data in the sinogram), and other uncorrected physical effects like scatter, lag, etc. Dosimetry results are summarized in Figure 3C. We see that the dynamic collimation scan was acquired with 57% of the dose of the fully sampled scan - indicating a significant potential for dose reduction.

Results from the thorax scan experiment are shown in Figure 4. In comparing the fully sampled scan with the two dynamic collimation protocols we see a similar level of image quality in the VOI that was chosen around the spine for all methods. As one would expect the 1:4 protocol has increased noise over both the 2:4 protocol and the fully sampled data. Interestingly, the ring artifacts are significantly reduced in the 2:4 protocol. We conjecture that the pairwise actuation of blockers eliminates the systematic omission of radial bins that are present in the singlet blocker opening, which reduces systematic ring artifacts. The image quality outside the VOI is better in the 2:4 protocol (over the 1:4 case) with its increased sampling.

### 4. CONCLUSION

In this work we have demonstrated a novel dynamic collimation approach based on the independent actuation of beam blockers placed along the radial direction of a CT scanner. The device was constructed, calibrated, and used to acquire projection data on a experimental test-bench. A model-based approach was developed to

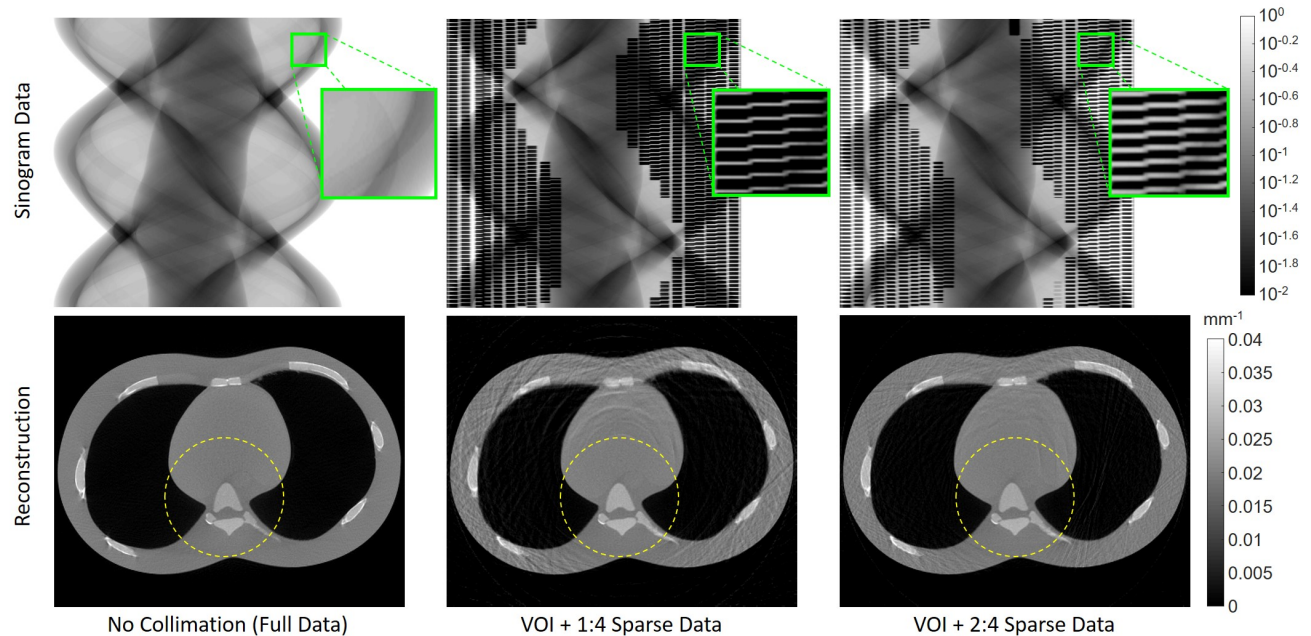


Figure 4. Summary of the thorax phantom experiment including fully sampled data and two different sparse sampling protocols: VOI+1:4 and VOI+2:4. Both sinogram data and the associated PWLS reconstruction are shown for each case. The circular VOI is shown as a yellow dashed circle in all volumes.

reconstruct data from acquisition protocols with variable sampling. We demonstrated the ability to maintain image quality within a VOI while significantly reducing radiation dose.

These preliminary studies show one potential use of the dynamic collimator to control image quality and limit dose. Much more general dynamic sampling patterns are possible. For example, we have illustrated how pairwise actuation can limit certain artifacts. A wide range of other image quality and dose objectives could also be applied including smoother variations in image quality (spatially), organ-by-organ specification, task-driven sampling, etc.

There are numerous engineering details that would need to be addressed to translate this approach to a clinical system including strict constraints on the motion (accelerations, velocity), overall size, control and communication, etc. However, these initial studies suggest that the underlying technology has potential to provide a new way to control and balance the image quality-dose trade-off.

## REFERENCES

- [1] Gies, M., Kalender, W. A., Wolf, H., Suess, C., Gies, M., Kalender, W. A., Wolf, H., Suess, C., Madsen, M. T., Gies, M., Kalender, W. A., Wolf, H., and Suess, C., "Dose reduction in CT by anatomically adapted tube current modulation. I. Simulation studies.," *Medical physics* **26**, 2248–2253 (nov 1999).
- [2] Shunhavanich, P., Hsieh, S. S., and Pelc, N. J., "Fluid-filled dynamic bowtie filter: a feasibility study.," *Proc. SPIE* **9412**, 94121L (2015).
- [3] Szczykutowicz, T. P. and Hermus, J., "Fluid dynamic bowtie attenuators.," *Proc. SPIE* **9412**, 94120X (2015).
- [4] Hsieh, S. S. and Pelc, N. J., "The feasibility of a piecewise-linear dynamic bowtie filter.," *Medical physics* **40**, 031910 (feb 2013).
- [5] Huck, S. M., Fung, G. S. K., Parodi, K., and Stierstorfer, K., "Technical Note: Sheet-based dynamic beam attenuator – A novel concept for dynamic fluence field modulation in x-ray CT.," *Medical Physics* (jul 2019).

- [6] Gang, G. J., Mao, A., Wang, W., Siewerdsen, J. H., Mathews, A., Kawamoto, S., Levinson, R., and Stayman, J. W., “Dynamic fluence field modulation in computed tomography using multiple aperture devices,” *Physics in Medicine and Biology* **64** (may 2019).
- [7] Szczykutowicz, T. P. and Mistretta, C. A., “Design of a digital beam attenuation system for computed tomography: part I. System design and simulation framework.,” *Medical physics* **40**(2), 021905 (2013).
- [8] Szczykutowicz, T. P. and Mistretta, C. a., “Design of a digital beam attenuation system for computed tomography. Part II. Performance study and initial results.,” *Medical physics* **40**(2), 021906 (2013).
- [9] Bian, J., Wang, J., Han, X., Sidky, E. Y., Shao, L., and Pan, X., “Optimization-based image reconstruction from sparse-view data in offset-detector CBCT.,” *Physics in medicine and biology* **58**, 205–30 (jan 2013).
- [10] Chen, B., Kobler, E., Muckley, M. J., Sodickson, A. D., O’Donnell, T., Flohr, T., Schmidt, B., Sodickson, D. K., and Otazo, R., “SparseCT: System concept and design of multislit collimators,” *Medical Physics* **46**, 2589–2599 (jun 2019).
- [11] Leong, A., Gang, G. J., Sisniega, A., Wang, W., Wu, J., Bambot, S. B., and Stayman, J. W., “An Investigation of Slot-scanning for Mammography and Breast CT,” *Proceedings of SPIE—the International Society for Optical Engineering* **11312**, 25 (mar 2020).
- [12] Bartolac, S., Graham, S., Siewerdsen, J. H., and Jaffray, D. A., “Fluence field optimization for noise and dose objectives in CT,” (2011).
- [13] Gang, G. J., Siewerdsen, J. H., and Stayman, J. W., “Task-driven optimization of fluence field and regularization for model-based iterative reconstruction in computed tomography,” *IEEE Transactions on Medical Imaging* **36**(12), 2424–2435 (2017).
- [14] Erdogan, H. and Fessler, J. A., “Ordered subsets algorithms for transmission tomography.,” *Physics in medicine and biology* **44**, 2835–51 (nov 1999).